Physicochem. Probl. Miner. Process., 62(4), 2026, 231190

http://www.journalssystem.com/ppmp

Physicochemical Problems of Mineral Processing

ISSN 1643-1049

Thermal treatment of granite quarry waste: Numerical integration–based thermal quality assessment and Bond Work Index (BWI) modelling

Ekin Köken [1], Ismail Ince [2], Hande Marulcuoğlu [1], Pawel Strzalkowski [3], Ahmet Özarslan [4]

[1] Abdullah Gül University, Materials Science and Nanotechnology Engineering Department, Kayseri – Türkiye

[2] Konya Technical University, Geological Engineering Department, Konya – Türkiye

[3] Wroclaw University of Science and Technology, Faculty of Geoengineering, Mining and Geology, Department of Mining, Wroclaw, Poland

[4] Zonguldak Bülent Ecevit University, Mining Engineering Department, Zonguldak - Türkiye

Corresponding author: ekin.koken@agu.edu.tr (Ekin Köken)

Abstract: This study investigates how thermal treatment up to 600 °C alters the physical, mechanical, and grindability properties of granite quarry waste materials, with a view to promoting their sustainable reuse. Seven representative wastes (R1–R7) from operating quarries in Türkiye were characterised through laboratory testing, and a conventional numerical integration approach was applied to quantify the thermal sensitivity of each property. Results show that no single waste material performed best across all rock properties, indicating that thermal pre-treatment must be application-specific and governed by the sensitivity of the property of interest. Grindability behaviour was assessed through Bond Work Index (BWI) tests and modelled using regression and soft-computing analyses. The study thus provides an experimental and computational decision framework, showing that thermal treatment can reduce the grinding energy demand of granite waste, while indicating that further investigation is needed to establish whether such treatment is economically advantageous prior to crushing and grinding.

Keywords: granite waste, thermal treatment, quality assessment, bond work index, sustainable mining

1. Introduction

Understanding the impact of thermal treatment on rock properties is critical for geo-engineering applications, such as geothermal energy extraction, deep underground coal gasification, enhanced oil recovery, wellbore stability, and nuclear waste disposal. Elevated temperatures induce micro/macro structural and geochemical alterations that typically degrade key engineering properties, including strength, elasticity, permeability, and thermal expansion (Ranjith et al. 2012; Ozguven and Ozcelik 2014; Zhang et al. 2016; Tian et al. 2017; Kumari et al. 2017, 2019; Rong et al. 2018; Wu et al. 2019; Zhang and Zhao 2020; Li et al. 2021; Vidana et al. 2021; Jin et al. 2024; Ram et al. 2025; Xu et al. 2025). Quantifying these variations is essential for evaluating the stability and performance of rock-based structures (Becattini et al. 2017; Aslannezhad et al. 2020; Dou et al. 2025). Furthermore, thermal pretreatment has been shown to reduce energy consumption and costs in mineral processing by facilitating ore comminution (Kingman et al. 2000; Purwanto et al. 2002; Cisternas et al 2022).

Thermal and microwave pretreatments significantly enhance comminution efficiency and mineral liberation. For instance, thermal pretreatment of bauxite and microwave heating of bastnaesite ore have been reported to reduce grinding energy requirements by 28% and 27%, respectively (Rao et al. 2002; Asgari et al. 2024). Beyond reducing energy consumption through thermal shock-induced micro-fracturing (Somani et al. 2017), heat treatment can improve concentrate grades; for example, conventional and microwave roasting of iron-rich ores have been shown to improve iron concentration by reducing gangue and phosphorus impurities (Omran et al. 2015).

DOI: 10.37190/ppmp/231190

Integrating thermal treatment with efficient waste-grinding systems offers a sustainable approach to resource recovery and volume reduction in rock aggregate manufacturing and ore-dressing operations. Primary and secondary crushing stages inevitably generate substantial volumes of fine waste material (Zheng et al. 2021). Characterizing the engineering properties of these by-products is essential for their industrial upcycling. Granite fines, an abundant by-product of rock crushing processes, exhibit significant engineering properties, including high strength, low abrasion resistance, and low water absorption. While granite quarrying causes environmental challenges, addressing granite waste in engineering applications mitigates disposal hazards and air pollution (Amulya et al. 2021; Danish et al. 2021; Strzałkowski et al. 2025).

Granite waste and powder have been widely studied for their potential to enhance material performance in a wide range of engineering applications. In geotechnical engineering, incorporating granite fines effectively stabilizes soils, improves the California Bearing Ratio (CBR), enhances soil plasticity, and mitigates swelling behavior in expansive soils (Soosan et al. 2005; Eltwati et al. 2020; Abdelkader et al. 2022; Shah et al. 2022). In construction materials, adding granite powder improves the durability of cementitious composites (Raghavendra et al. 2015; Medina et al. 2017; Gupta and Vyas 2018; Xiao and Xu 2019; Ramadji et al. 2020) and serves as a practical component in autoclaved aerated concrete mixtures (Zafar et al. 2020). Furthermore, granite waste has demonstrated efficiency as a precursor in geopolymer synthesis (Tchadjié et al. 2016), as an additive to enhance the strength and sinterability of ceramics (Lu et al. 2019), and as a filler to optimize polymer composite properties (Tawfik et al. 2022). Apart from these, it has also been utilized as a nutrient source to regulate acidic soils (Silva et al. 2005).

Given the above explanations, it can be argued that using granite fines is advantageous from multiple perspectives. However, grinding rocks is labour-intensive and costly, and some efforts have been made to improve the efficiency of rock comminution processes. One well-established method for reducing physical and mechanical properties of rocks is thermal treatment (Zhang et al. 2009; Singh et al. 2019; Adewuyi et al. 2020). Thermal treatment can be applied to rock materials in two ways. One method involves directly heating rocks or ores in high-temperature furnaces (Vishal et al. 2011; Gautam et al. 2018; Yin et al. 2021; Zhu et al. 2022; Zhang et al. 2022), while the other employs an indirect approach based on microwave heating (Nejati 2014; Motlagh 2015; Hassani et al. 2016; Kahraman et al. 2020; Yang et al. 2025).

Although the thermal degradation of rock properties is well established, utilizing this effect to aid rock comminution can yield notable economic and sustainability benefits in engineering sciences and waste management. Prior research extensively describes how heated intact rocks weaken physically and mechanically, including reductions in Uniaxial Compressive Strength (UCS) and ultrasonic velocity, along with increased porosity caused by dehydration, differential thermal expansion, and grain boundary damage (Lin 2002; Griffiths et al. 2017; Tomás et al. 2021; Kahraman 2022; Paul et al. 2022; Gomah et al. 2024). However, few studies address how rock waste responds thermally or how this affects grinding properties.

To address this gap in the waste management literature, this study explores the physical, mechanical, and grinding characteristics of granite quarry waste after controlled thermal treatment. While it does not claim to present new findings on individual weakening trends in selected rock properties, its main contributions are: (1) a combined evaluation of granite waste materials under elevated temperatures, (2) a quantification of their thermal quality by proposing a quantitative measure based on a numerical integration method, (3) possible relationships between rock mineralogy and their thermal response and (4) the development of novel predictive models to assess the grinding properties of these materials.

It is hypothesised that controlled thermal pretreatment induces microstructural thermal cracking and grain-boundary weakening, thereby enhancing comminution efficiency and reducing operational energy consumption. For this purpose, representative granite waste samples were collected from operational rock quarries in Türkiye. Cubical rock specimens were prepared and thermally treated to quantify changes in physical, mechanical, and grinding properties. Based on X-ray diffraction analyses, potential correlations are sought to explain the effects of thermal treatment on each granite waste material. In the subsequent sections, the thermal quality of these materials is quantified using a simple numerical integration method. Decay functions are developed to precisely reveal the effects of thermal treatment on selected rock properties, and regression and soft computing analyses are conducted to understand their grinding behaviour as a function of various inputs.

2. Materials and methods

2.1. Waste material collection

Representative waste rock blocks and rock aggregates with varying particle sizes were obtained from various rock quarry dump sites in Türkiye. Seven granite rock samples (R1–R7) were considered in this study. The sampling sites for granite waste materials are shown in Fig. 1.

2.2. Sample preparation and testing methods

The rock blocks were washed with distilled water to remove dust and other impurities. First, the mineralogical characterisation of the waste materials was carried out using rock powder samples (< 0.074 mm). A Bruker Discover D8 diffractometer with a Cu Kα_1 radiation source (λ = 1.54060 Å) was utilised for X-ray diffraction (XRD) analyses. The XRD patterns were analysed using HighScore Plus (ver. 3.0), which incorporated the second powder diffraction file (PDF-2 2011) and the Crystallography Open Database (COD 2016).

Based on the provided information, typical XRD patterns for each waste material are shown in Fig. 2. From these patterns, the relative abundance of rock-forming minerals was determined semi-quantitatively (Table 1).

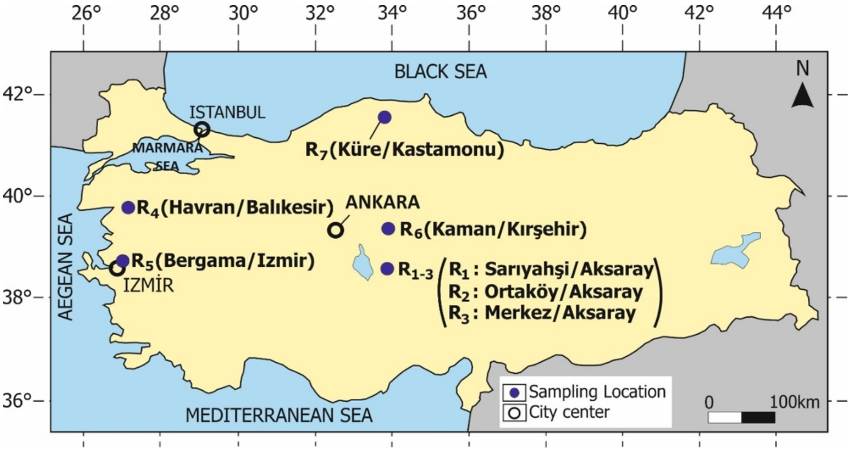

Fig. 1. Sampling locations of the granite waste materials

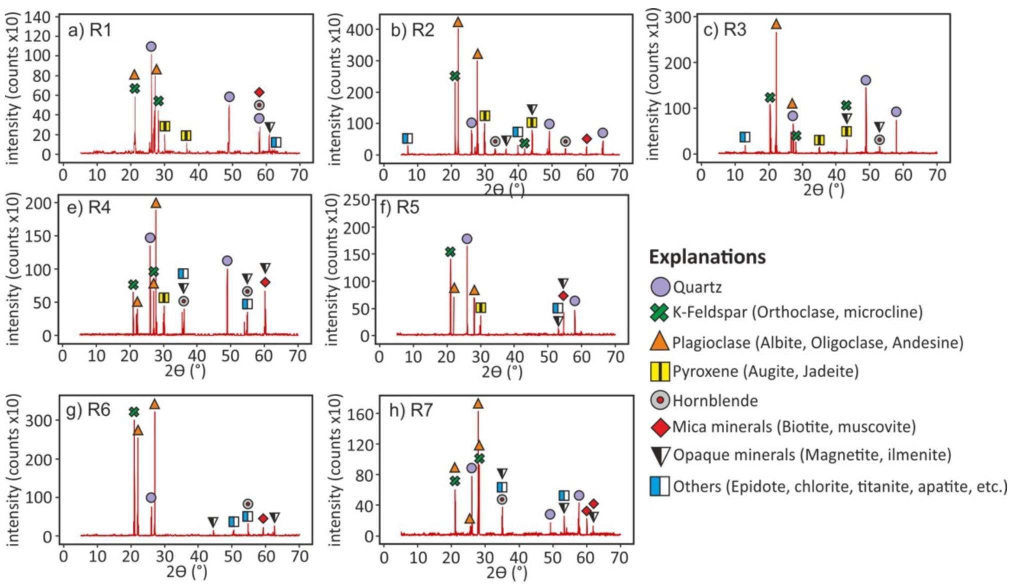

Fig. 2. Typical XRD patterns of the granite waste materials

Table 1. Mineralogical composition of the granite waste materials (semiquantitative)

Rock-forming mineral	R1	R2	R3	R4	R5	R6	R7
Quartz (wt. %)	37.3	13.4	16.6	29.5	34.1	7.2	24.5
Alkali Feldspar (K-Feldspar) (wt.% %)	14.2	17.1	16.3	12.3	22.9	28.5	16.4
Plagioclase (wt. %)	29.4	47.9	48.6	32.5	29.3	54.5	41.9
Pyroxene (wt. %)	7.00	9.5	7.3	5.4	5.6	<1	<1
Hornblende (wt. %)	4.4	2.5	<1	5.6	<1	2.3	3.7
Biotite (wt. %)	1.6	<1	<1	4.7	3.7	1.5	3.5
Muscovite (wt. %)	<1	<1	<1	2.3	1.8	<1	<1
Opaque minerals[1] (wt. %)	4.5	1.3	6.7	4.0	2.2	3.7	4.5
Others[2] (wt. %)	1.1	6.5	2.7	3.4	<1	2.1	4.4
Total (%)	99.75	100.20	100.34	99.70	100.65	101.34	100.90

Explanations: [1]Magnetite, ilmenite [2]Epidote, chlorite, titanite, apatite

Later, the rock blocks were cut and smoothed to obtain cubic samples in 70x70x70 mm dimensions. The physical properties considered in this study were dry density (ρ_d), effective porosity (n_e), and pulse wave velocity (V_p), while the mechanical property was uniaxial compressive strength (UCS). All tests described herein were carried out in accordance with the standards listed in Table 2.

To determine the grinding properties of the waste materials, Bond Work Index (BWI) tests were conducted in accordance with the procedures outlined by Bond (1961). For this purpose, 700 cm^3 of rock materials with a −3.35 mm size fraction was prepared for each rock type. The particle size distribution (PSD) of the prepared rock samples is shown in Fig. 3.

Table 2. Testing procedures employed in this study

Rock property	Dry density, ρ_d	Effective porosity, n_e	Pulse wave velocity, V_p	Uniaxial compressive strength, UCS
Testing apparatus	Precise balance Drying oven	Precise balance Drying oven Saturation water tank	E48 Pulse Generator with two transducers (54 kHz)	Stiff loading machine (2000 kN)
Standard	ASTM C97/C97M (2009)		ASTM E494 (2020)	ASTM C170 / C170M (2017)
Repetition	Five times before and after each thermal treatment	Five times before and after each thermal treatment	Ten measurements from each surface	Five times before and after each thermal treatment

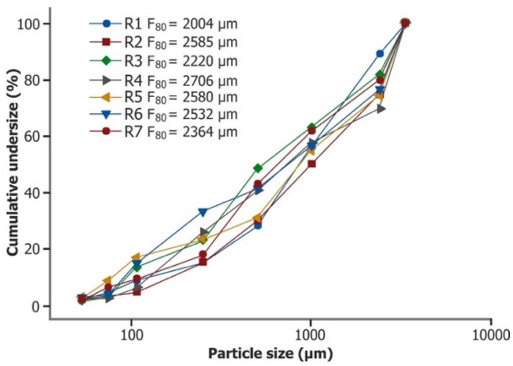

Fig. 3. Typical PSDs of the investigated granite waste materials

At temperatures of 25, 100, 200, 300, 400, 500 and 600 °C, the physical, mechanical and grinding properties of each granite waste material were determined. The heating rate in the high-temperature furnace was 5°C/min. After the target temperature was reached, the rock samples were held at this temperature for the next two hours. They were then left in the furnace to cool naturally. The laboratory tests were conducted under oven-dried conditions, and the descriptive statistics for each rock property were recorded. Average values of each rock property were used in soft computing analyses. The experimental workflow and analytical steps are summarized in Fig. 4.

The heating-cooling schedule was intended to represent a controlled laboratory pre-treatment rather than an optimised industrial heating process. A moderate heating rate of 5 °C/min, a 2 h soaking period, and natural cooling were systematically applied to mitigate thermal shock and provide an objective engineering interpretation.

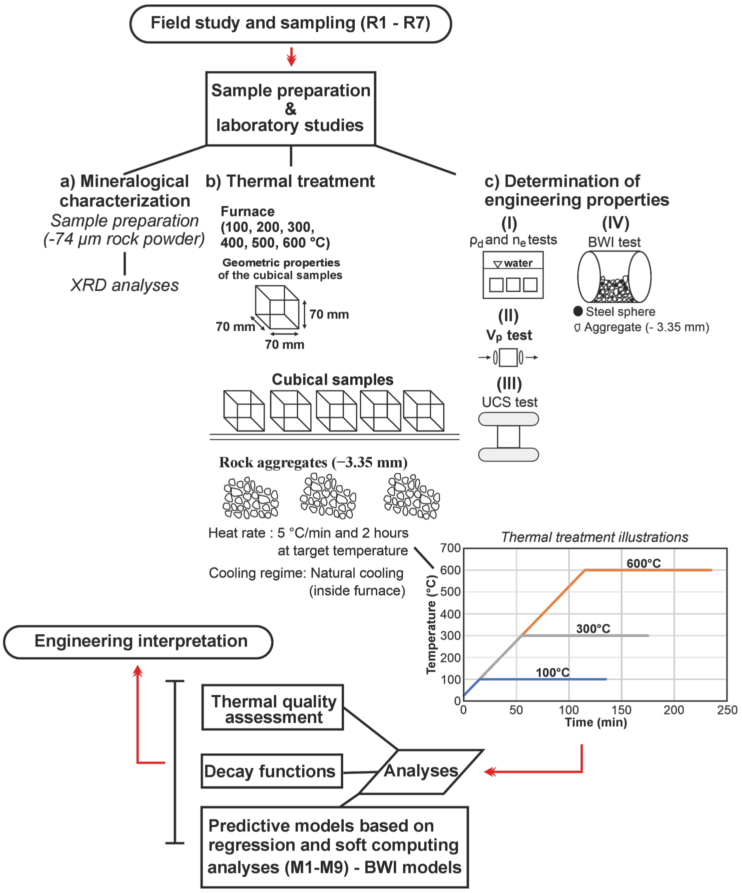

Fig. 4. Flowchart of the experimental procedure and study outline

2.3. Thermal quality assessment

Within this framework, the term "thermal quality" is defined as an operational evaluation metric rather than a universal material constant. It quantifies the cumulative degradation or deviation of a specific rock property from its room-temperature baseline across the temperature range under investigation. Consequently, this metric is a comparative, repeatable quantity derived directly from laboratory test results.

The influence of thermal treatment on rock engineering properties was quantified using numerical integration (Trapezoidal rule). After plotting each rock property as a function of temperature (T), the area (A_e) beneath the response curve f(T) was used as a reliable measure of thermal impact. In the hypothetical absence of thermal effects (no thermal effects are available), this area would equal a constant baseline (A_e=A_0).

In practice, a typical increase is observed in the considered area when n_e is considered (Fig. 5a), whereas it decreases for other rock properties, for example, ρ_d, V_p and UCS values (Fig. 5b). Based on these changes in Ae, the thermal quality of the waste materials was assessed and compared to one another. Accordingly, the area beneath the response curve was calculated using Eqs. 1 and 2.

$$\text{Enclosed area } (A_e) = \int_a^b (f_x)dx \approx \frac{h}{2}\left[f(x_0) + 2\sum_{i=1}^{n-1} f(x_i) + f(x_n)\right] \quad (1)$$

$$h = \frac{b-a}{n} = \frac{\Delta T}{n} \quad (2)$$

where a and b are the start and end points (or start/end temperatures), and n is the number of intervals.

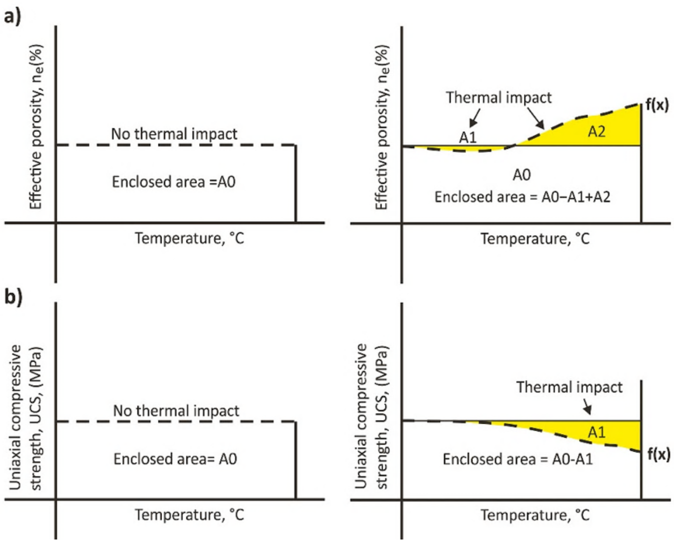

Fig. 5. Thermal effects on different rock properties: a) Effective porosity, b) Uniaxial compressive strength

To assess the thermal quality of each waste material, the calculated Ae was compared with the theoretical baseline with no thermal effect (A0 = Tmax × maximum value of the adopted rock property (Pmax)). This comparison provides a practical, reliable metric for evaluating the thermal quality of waste materials.

3. Laboratory studies

Cubic samples were saturated in a water tank containing distilled water at 21 ± 1 °C for 24 hours. The saturated weights (Ws) of the samples were recorded on a precision balance. The samples were then oven-dried at 105 °C ± 2 °C for 24 hours to obtain dry weights (Wd). Subsequently, ρd and ne were calculated using Eqs. 3 and 4, respectively.

$$\rho_d = \frac{W_d}{V} \quad (3)$$

$$n_e = \frac{\frac{W_s - W_d}{\rho_w}}{V} \times 100 \quad (4)$$

where W_d: Oven-dried weight of the cubical sample (g), W_s: Saturated weight of the cubical sample (g), ρ_w: density of distilled water (1 g/cm^3), V: Volume of the cubical sample (cm^3).

A servo-controlled stiff-loading machine (capacity: 2000 kN) was used to determine the UCS of the samples at loading rates of approximately 0.5–1.0 MPa/s. The V_p of each rock sample was measured using an E48 Pulse Generator testing apparatus. The BWI tests were carried out using a standard ball mill (ball mill width: 30.48 cm, ball mill length: 30.48 cm, number of mill rotations: 70 rpm, total volume of the ball mill: 700 cm^3, ball charge ratio: 40%). The BWI index tests were completed once the circulating load reached 250%. BWI values were then calculated using Eq. 5. Typical laboratory studies are illustrated in Fig. 6.

$$\text{BWI} = \frac{44.5}{{P_{test}}^{0.23} \times G^{0.82} \times \left(\frac{10}{\sqrt{P_{80}}} - \frac{10}{\sqrt{F_{80}}}\right)} \quad (5)$$

where BWI is the Bond Work Index (kWh/t), Ptest is the test sieve size (106 µm in this study). G is the grindability ratio (g/rev), P80 is the characteristic product size (µm) at which 80% of the total product is undersized, and F80 is the characteristic feed size (µm) at which 80% of the feed is undersized.

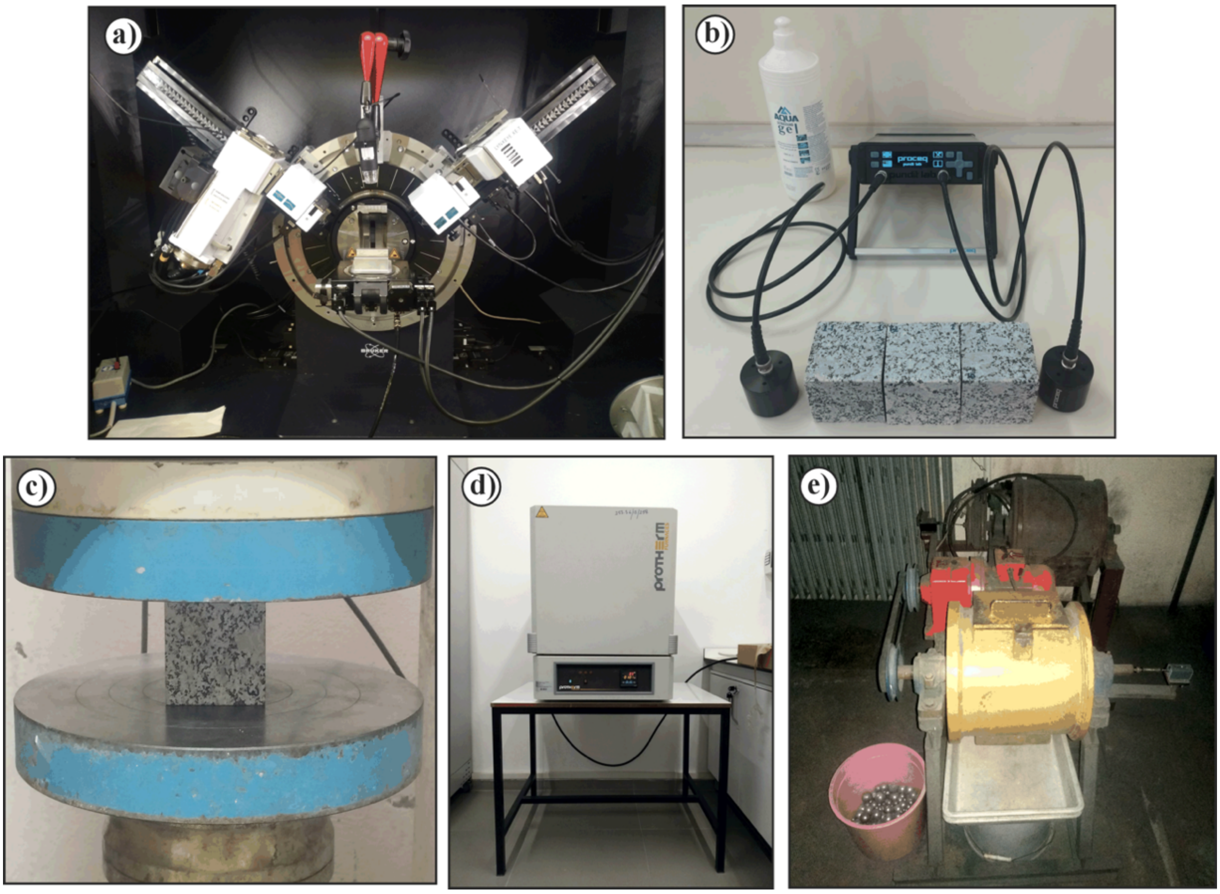

Fig. 6. Laboratory studies: a) XRD analysis b) Pulse wave velocity measurement c) UCS test, d) High-temperature furnace used in thermal treatment, e) BWI test

4. Results and discussion

4.1. Impacts of thermal treatment on adopted rock properties

Rock materials undergo both physical and chemical transformations when exposed to high temperatures. Physically, they lose water, leading to changes in mass and volume, and develop microcracks due to differences in thermal expansion among minerals (Zhang et al. 2016). Chemically, they may undergo phase transitions in crystals and deterioration at grain boundaries. These internal and external structural signs indicate diverse responses that depend on the rock's physical and mechanical properties.

From a detailed thermomechanical perspective, owing to the different thermal expansion coefficients of rock-forming minerals, heating and cooling cycles produce non-uniform volumetric strains (Helgeson 1978; Zaraisky and Balashov 1994; Siegesmund et al. 2018; Le Pape et al. 2018; Wang et al. 2020) that promote microcrack initiation at grain boundaries, thereby reducing rock strength properties.

Furthermore, temperature-induced phase transformations in rock-forming minerals can trigger thermogravimetric changes, such as dehydration, decarbonisation, and dihydroxylation, which can lead to microcracks that further weaken structural integrity (Wu et al. 2019; Vidana Pathiranagei et al. 2021; Ram et al. 2025).

As summarized above, Table 3 presents descriptive statistics on variations in rock properties under thermal treatment. The laboratory test results indicate that the average UCS values at 25 °C ranged from 70.90 to 182.57 MPa, whereas after heating to 600 °C, they decreased to 28.68–146.30 MPa. These decreases correspond to thermally induced microcracking and increased porosity, which weaken the samples' internal structure. Variations in V_p values also support the temperature-induced reduction in structural integrity of rock samples. Consistent with thermally induced microcracking, V_p decreased as temperature increased, while n_e showed a gradual increase.

Table 3. Physical, mechanical and grinding properties of granite waste materials.

Waste material	T (°C)	ρ_d (g/cm^3)	n_e (%)	V_p (km/s)*	UCS (MPa)	BWI (kWh/t)**	Strength classification***	Porosity classification***	Crushability classification***
							(Deere and Miller (1966)	Anon (1979)	Metso (2011)
R1	25	2.681 ± 0.089 (10)	0.35 ± 0.016 (10)	5.06 ± 0.227 (10)	162.7 ± 25.28 (5)	17.95 ± 1.20 (3)			
	100	2.675 ± 0.06 (4)	0.44 ± 0.025 (4)	4.93 ± 0.71 (4)	160.91 ± 18.57 (4)	16.59 ± 0.49 (3)			Class II
	200	2.665 ± 0.10 (3)	0.45 ± 0.039 (3)	4.66 ± 0.42 (3)	157.22 ± 22.11 (3)	15.54 ± 0.68 (3)	Class II		
	300	2.652 ± 0.04 (4)	0.51 ± 0.056 (4)	4.47 ± 0.28 (4)	151.5 ± 15.07 (4)	15.37 ± 1.92 (3)		Class I	
	400	2.639 ± 0.12 (3)	0.54 ± 0.063 (3)	4.43 ± 0.52 (3)	147.05 ± 11.14 (3)	15.05 ± 1.04 (3)			Class II - Class III
	500	2.625 ± 0.05 (3)	0.62 ± 0.034 (2)	4.22 ± 0.28 (2)	125.57 ± 8.35 (2)	14.89 ± 0.87 (3)			
	600	2.617 ± 0.05 (3)	0.68 ± 0.030 (2)	4.10 ± 0.15 (2)	109.5 ± 13.79 (2)	14.58 ± 0.63 (3)	Class II - Class III		
R2	25	2.61 ± 0.075 (6)	0.56 ± 0.091 (6)	4.11 ± 0.19 (6)	145.2 ± 4.19 (5)	16.25 ± 0.50 (3)		Class I	
	100	2.61 ± 0.044 (6)	0.63 ± 0.137 (6)	4.04 ± 0.12 (6)	146.17 ± 9.06 (5)	16.21 ± 0.84 (3)			Class II
	200	2.60 ± 0.057 (6)	0.93 ± 0.314 (6)	3.95 ± 0.17 (6)	138.5 ± 4.54 (5)	15.82 ± 1.37 (3)	Class II	Class I - Class II	
	300	2.59 ± 0.035 (4)	1.21 ± 0.265 (4)	3.74 ± 0.31 (4)	136.5 ± 6.62 (5)	14.99 ± 1.76 (3)			
	400	2.59 ± 0.055 (4)	1.6 ± 0.71 (4)	3.39 ± 0.19 (4)	127.4 ± 10.55 (5)	14.66 ± 1.37 (3)			Class II - Class III
	500	2.58 ± 0.061 (3)	1.76 ± 0.53 (3)	3.05 ± 0.30 (3)	106.2 ± 10.84 (5)	14.02 ± 0.62 (3)	Class II - Class III	Class II	
	600	2.569 ± 0.027 (3)	1.8 ± 0.34 (3)	2.76 ± 0.08 (3)	98.3 ± 17.81 (5)	13.65 ± 0.98 (3)			
R3	25	2.57 ± 0.024 (5)	1.07 ± 0.36 (5)	4.39 ± 0.094 (5)	138.40 ± 8.82 (3)	15.69 ± 1.42 (3)			Class II
	100	2.574 ± 0.059 (4)	1.08 ± 0.24 (4)	4.42 ± 0.13 (4)	140.71 ± 5.87 (3)	15.05 ± 1.22 (3)		Class I - Class II	
	200	2.569 ± 0.033 (4)	1.23 ± 0.71 (4)	4.34 ± 0.19 (4)	140.26 ± 11.97 (3)	14.57 ± 0.74 (3)	Class II		
	300	2.551 ± 0.047 (3)	1.49 ± 0.59 (3)	4.22 ± 0.074 (3)	134.25 ± 18.04 (3)	13.39 ± 0.55 (3)			Class II - Class III
	400	2.533 ± 0.066 (3)	1.94 ± 0.24 (3)	3.86 ± 0.21 (3)	125.29 ± 11.63 (3)	12.59 ± 0.81 (3)			
	500	2.513 ± 0.017 (3)	2.11 ± 0.48 (3)	3.71 ± 0.14 (3)	112.26 ± 15.70 (3)	12.44 ± 1.54 (3)	Class II - Class III	Class II	
	600	2.475 ± 0.024 (3)	2.33 ± 0.85 (3)	3.56 ± 0.065 (3)	104.71 ± 5.35 (3)	10.6 ± 2.05 (3)			Class III - Class IV
R4	25	2.702 ± 0.030 (7)	0.76 ± 0.25 (7)	4.28 ± 0.10 (7)	144.32 ± 21.80 (7)	17.90 ± 1.35 (4)			
	100	2.704 ± 0.027 (6)	0.75 ± 0.14 (6)	4.28 ± 0.014 (6)	147.72 ± 15.35 (6)	17.66 ± 0.82 (4)			Class II
	200	2.695 ± 0.034 (6)	0.96 ± 0.28 (6)	4.12 ± 0.050 (6)	134.4 ± 16.22 (6)	17.2 ± 1.60 (4)	Class II	Class I - Class II	
	300	2.685 ± 0.026 (4)	1.2 ± 0.38 (4)	3.46 ± 0.32 (4)	130.44 ± 27.61 (4)	16.53 ± 2.68 (4)			
	400	2.662 ± 0.046 (3)	1.27 ± 0.60 (3)	3.15 ± 0.40 (3)	123.25 ± 9.50 (3)	16.02 ± 1.05 (4)			Class II - Class III
	500	2.615 ± 0.029 (3)	1.47 ± 0.46 (3)	2.64 ± 0.15 (3)	115.82 ± 17.80 (3)	15.47 ± 1.73 (3)	Class II - Class III		
	600	2.584 ± 0.024 (3)	1.93 ± 0.51 (3)	2.61 ± 0.11 (3)	109.66 ± 11.50 (3)	14.97 ± 0.81 (3)		Class II	

Table 3. Physical, mechanical and grinding properties of granite waste materials (continued)

Waste material	T (°C)	ρ_d (g/cm^3)	n_e (%)	V_p (km/s)*	UCS (MPa)	BWI (kWh/t)**	Strength classification***	Porosity classification***	Crushability classification***
							(Deere and Miller (1966)	Anon (1979)	Metso (2011)
R5	25	2.741 ± 0.019 (7)	0.52 ± 0.15 (7)	5.37 ± 0.22 (7)	182.57 ± 14.06 (4)	21.66 ± 1.52 (3)	Class II	Class I	Class I
	100	2.742 ± 0.030 (5)	0.49 ± 0.24 (5)	5.21 ± 0.40 (5)	179.21 ± 18.10 (4)	21.15 ± 1.08 (3)			
	200	2.743 ± 0.036 (4)	0.56 ± 0.18 (4)	4.87 ± 0.51 (4)	173.96 ± 9.32 (3)	20.65 ± 1.18 (3)			
	300	2.726 ± 0.054 (5)	0.74 ± 0.27 (5)	4.53 ± 0.35 (5)	165.42 ± 14.39 (3)	19.8 ± 1.91(3)		Class I - Class II	Class I - Class II
	400	2.71 ± 0.044 (4)	0.93 ± 0.38 (4)	4.24 ± 0.25 (3)	162.27 ± 10.08 (3)	18.45 ± 1.49 (3)			
	500	2.676 ± 0.041 (4)	1.37 ± 0.23 (4)	4.22 ± 0.290 (4)	150.72 ± 9.86 (3)	18.14 ± 1.88 (3)		Class II	
	600	2.635 ± 0.017 (3)	1.62 ± 0.49 (3)	4.12 ± 0.220 (3)	146.3 ± 8.490 (3)	17.75 ± 1.10 (3)			
R6	25	2.68 ± 0.012 (4)	0.65 ± 0.40 (4)	4.32 ± 0.170 (4)	109.37 ± 16.82 (3)	17.85 ± 2.45 (3)	Class II - Class III	Class I - Class II	Class I - Class II
	100	2.675 ± 0.025 (4)	0.97 ± 0.31 (4)	4.24 ± 0.204 (4)	104.14 ± 20.60 (3)	17.02 ± 1.52 (3)			
	200	2.662 ± 0.018 (5)	1.23 ± 0.27 (5)	4.17 ± 0.153 (5)	96.21 ± 14.72 (3)	15.47 ± 1.65 (3)			Class II - Class III
	300	2.652 ± 0.041 (4)	1.57 ± 0.55 (4)	4.09 ± 0.314 (3)	90.07 ± 25.13 (3)	15.25 ± 2.21 (3)		Class II	
	400	2.649 ± 0.053 (4)	1.96 ± 0.32 (4)	3.41 ± 0.126 (4)	85.34 ± 9.26 (3)	14.39 ± 1.73 (3)			
	500	2.631 ± 0.027 (3)	2.43 ± 0.72 (3)	3.05 ± 0.238 (3)	74.88 ± 13.06 (3)	13.6 ± 0.54 (3)			
	600	2.584 ± 0.019 (3)	2.51 ± 0.59 (3)	2.96 ± 0.092 (3)	62.78 ± 8.52 (3)	12.71 ± 1.03 (3)	Class III - Class IV		Class III
R7	25	2.610 ± 0.034 (7)	0.88 ± 0.26 (7)	3.96 ± 0.074 (7)	70.90 ± 12.52 (3)	14.62 ± 0.88 (3)	Class III	Class I - Class II	Class II - Class III
	100	2.586 ± 0.022 (5)	1.23 ± 0.40 (5)	3.85 ± 0.118 (5)	58.95 ± 10.09 (3)	13.48 ± 1.53 (3)	Class III - Class IV		
	200	2.580 ± 0.037 (5)	1.58 ± 0.71 (5)	3.54 ± 0.304 (5)	51.01 ± 6.22 (3)	12.47 ± 2.36 (3)			Class III - Class IV
	300	2.571 ± 0.015 (4)	2.21 ± 0.44 (4)	3.26 ± 0.102 (4)	50.22 ± 9.20 (3)	10.32 ± 0.53 (3)			
	400	2.564 ± 0.038 (4)	3.17 ± 1.09 (4)	3.14 ± 0.247 (4)	47.26 ± 10.43 (3)	8.91 ± 1.06 (3)			Class IV
	500	2.511 ± 0.011 (3)	4.31 ± 1.64 (3)	2.9 ± 0.183 (3)	39.84 ± 10.70 (3)	8.25 ± 0.73 (3)	Class IV	Class II - Class III	
	600	2.459 ± 0.023 (4)	5.71 ± 0.99 (4)	2.72 ± 0.114 (4)	28.68 ± 7.68 (3)	7.54 ± 0.40 (3)			

Note: The notation of 2.741 ± 0.019 (7) indicates the average ± standard deviations (number of individual samples)

Note: *Considering each surface of the cubic samples, V_p measurements have been conducted.

Note: **BWI test has been conducted using individual rock aggregate samples (−3.35 mm).

Note: ***Rock material classifications adopted are given in Table 4.

DOI: 10.37190/ppmp/231190

On the other hand, the decrease in BWI values can be attributed to the increased grindability of rock at higher temperatures. In line with the scientific evidence of the relationship between rock strength and BWI (Aras 2009; Haffez 2012; Aras et al. 2020; Ranjbar et al. 2021), the R7 sample, which exhibited the greatest reduction in BWI at 600°C among all materials, also has lower rock strength properties.

For example, the grinding process for thermally treated R7 can be performed with less energy. From another perspective, the strength, porosity, and crushability classifications of the granite waste materials were also demonstrated using the quantitative approaches proposed by Deere and Miller (1966), Anon (1979), and Metso (2011), respectively (Table 4). Because the adopted rock material classifications provide only indirect information on the thermal quality of the granite wastes, the following section presents a novel method to quantify this quality.

Table 4. Rock material classifications based on different inputs

Strength classification		Porosity classification		Crushability classification	
Deere and Miller (1966)		Anon (1979)		Metso (2011)	
UCS (MPa)	Class	n_e (%)	Class	BWI (kWh/t)	Crushability
< 25	Very weak (V)	<1	Very low (I)	<7	Very easy (V)
25–50	Weak (IV)	1–5	Low (II)	7–10	Easy (IV)
50–100	Moderate (III)	5–15	Moderate (III)	10–14	Moderate (III)
100–200	Hard (II)	15–30	High (IV)	14–18	Difficult (II)
> 200	Very hard (I)	>30	Very high (V)	>18	Very difficult (I)

4.2. Thermal quality quantification

Temperature-dependent variations in the selected rock properties were quantified using Eqs. 1 and 2. The A_e beneath each response curve in Fig. 7 was calculated using the Trapezoidal rule. Using Ae and A0 together, a new rating point (RP) was assigned to each rock type using Eq. 6.

$$\mathrm{RP} = \frac{A_0 - A_e}{100} \tag{6}$$

where A_0: Theoretical baseline ($A = T_{max} \times P_{max}$), A_e: Area beneath the response curve.

RP is a dimensionless index quantifying the relative change from A_0 to Ae; it therefore represents a normalised ratio rather than a physical quantity with units. Dividing by 100 in Eq. 6 simplifies calculation and interpretation of the index. For rock properties that decrease with temperature (e.g., UCS and BWI), a higher RP value indicates lower thermal quality of granite waste. Conversely, for properties that increase with temperature, such as n_e, a lower RP value indicates higher thermal quality.

To facilitate calculations, a user-friendly MATLAB code was developed to determine RP for each waste material. Fig. 7 illustrates some RPs of waste materials in relation to different rock properties. For example, based on ρd, R6's RP (0.84) is lower than R4's (0.90), suggesting that R6 has higher thermal quality. Regarding the R1 material, the best thermal performance is shown, with an RP of 1.10. Likewise, R3 (RP = 16.8) appears to perform better than R6 (RP = 20.45) when considering their BWI variations (see Table 5). These comparisons can also be made easily using the lab test results in Table 3. In general, Table 5 enables a straightforward assessment of the thermal performance of granite waste materials in relation to their physical and mechanical properties. It also provides strong evidence for analyzing their engineering behaviour under different temperature conditions.

In other words, conventional thermal treatment does not affect different rock properties uniformly. Therefore, the thermal quality of granite wastes varies with both elevated temperature and rock properties. This highlights that a single thermal resistance cannot be assigned to these materials.

Within this framework, numerical integration techniques provide a systematic, quantitative basis for evaluating and comparing the thermal quality of granite waste. These methods capture the cumulative effects of thermal treatment on commonly used rock parameters, namely ρ_d, n_e, V_p, and UCS.

Furthermore, examining the relationships between the thermal quality indices (RPs) derived from various rock properties and selected physical and mechanical characteristics indicates that the indices based on ne and BWI show a relatively stronger association with UCS at room temperature. Conversely, BWI-based thermal quality of granite waste materials cannot be reliably assessed using their initial V_p

values. This suggests that although elastic wave characteristics reflect the degree of structural heterogeneity within rock materials, they are less effective indicators of thermal degradation behaviour in this context (Fig 8).

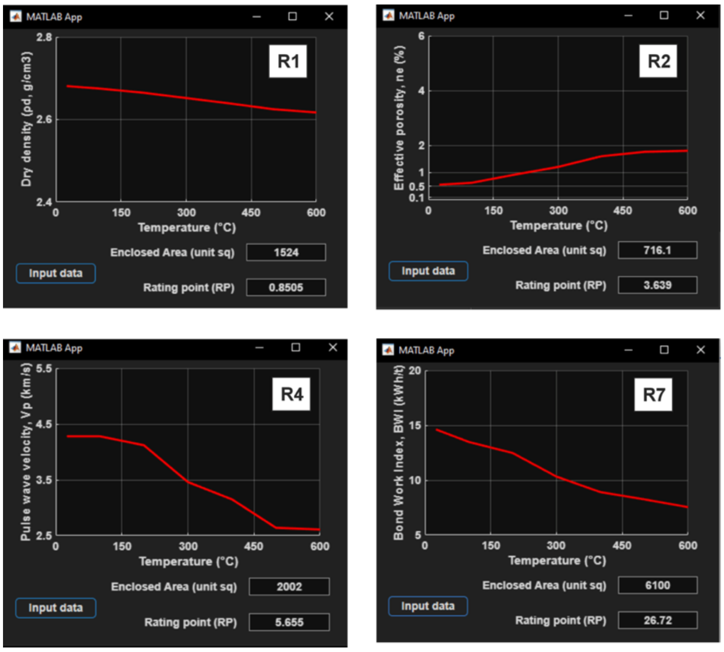

Fig. 7. Numerical integration examples for assessing the variations in rock properties in relation to thermal treatment

Table 5. Relative quality of waste materials concerning different rock properties.

Physical properties			Mechanical properties	Grinding properties	Thermal quality
ρ_d	n_e	V_p	UCS	BWI	Best
R2	R1	R3	R3	R2	
R3	R2	R2	R2	R4	
R6	R5	R1	R1	R3	
R1	R3	R6	R4	R5	
R5	R4	R7	R5	R1	
R4	R6	R4	R7	R6	
R7	R7	R5	R6	R7	Worst

Note: Thermal quality of granite wastes has been evaluated based on the RPs calculated using Eq 6.

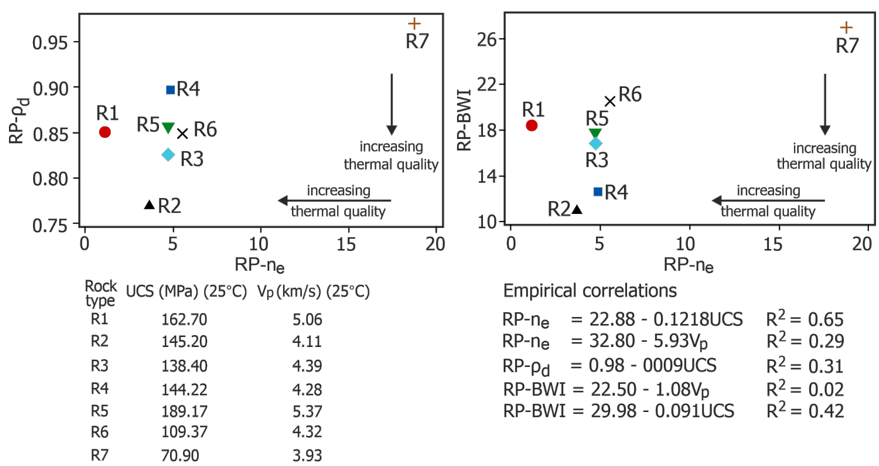

Fig. 8. Assessment of RPs concerning some rock properties at room temperature

It also seems logical that the thermal response of granite waste is influenced by mineralogical variations. Several researchers (Liu et al. 2016; Siegesmund et al. 2018; Paul et al. 2022; Lasheen et al. 2023; Abddaim et al. 2024; Alzo'ubi and Alneasan 2025) concluded that rock mineralogy significantly influences thermal expansion, permeability, and microstructural sensitivity. In this context, correlation analyses were conducted to assess the potential impact of mineralogical composition on the thermal resistance of granite waste materials. Table 6 summarizes these relationships. The V_p-based thermal quality of the granite waste materials exhibits a moderate positive association with Qtz content and a moderate negative association with Plg content (r = 0.545 and r = −0.653, respectively), consistent with the theoretical and practical framework proposed by Helgeson (1978). However, given the limited sample size (n = 7), neither correlation is statistically significant (p = 0.205 and p = 0.112, respectively). Accordingly, these trends should be regarded as preliminary observations rather than as a reliable basis for engineering decision-making. Given the limited number of granite waste samples examined in this study (n=7), future research is recommended to investigate how mineralogical variability influences the thermal quality of granite waste from additional perspectives, such as abrasion and fragmentation resistance, using more comprehensive datasets encompassing a broader range of granite sources. Such studies would help establish whether the observed trends are statistically significant.

Table 6. Pearson’s correlation matrix of mineralogical features and thermal changes in different properties

Parameter	Qtz	K−feld	Plg	Pearson’s correlation coefficient, r	Correlation degree **
RP (ρ_d)	0.360 (0.428)	−0.165 (0.724)	−0.290 (0.528)	0	No correlation
RP (n_e)	−0.090 (0.848)	−0.014 (0.977)	0.174 (0.709)	0 – 0.20	Very weak
RP (V_p)	**0.545** (0.205)	0.045 (0.924)	**−0.653** (0.112)	0.21 – 0.40	Weak
RP (UCS)	0.226 (0.627)	0.264 (0.567)	−0.309 (0.500)	0.41 – 0.60	Moderate
RP (BWI)	0.038 (0.936)	0.270 (0.558)	0.098 (0.835)	0.61 – 0.80	Strong
				0.81 – 0.99	Very strong
				1	Perfect

* Bold values indicate correlations of moderate strength or higher (|r| ≥ 0.41), regardless of statistical significance, given the limited sample size.
**Adapted from Landis and Koch (1977). P-values are shown in parentheses.

4.3. Decay functions

When evaluating cycling or progressive hazard assessment of rocks or rock-related structures, decay functions are primarily used to understand their long-term behaviour. Incorporating decay functions into the modelling of the progressive deterioration of rock materials also helps identify critical points at which the materials become unstable in terms of their physical and mechanical properties. Although decay functions have mainly been used to assess cyclic freeze–thaw impacts on rock materials (Mutlutürk et al. 2004; Jamshidi et al. 2013; Aral et al. 2021; Huang et al. 2025), they can also be utilized when assessing incremental heating or heating-cooling processes. Based on laboratory test results conducted under controlled heating conditions, various decay functions were derived for the selected inputs. The typical form of the decay function in rock engineering is given by Eq. 7. The specific decay functions are listed in Table 7.

The decay constant (d_c) for ρ_d ranged from -7.74×10^{-5} to -2.43×10^{-5}, with an average of -4.72×10^{-5}. Similarly, for BWI, d_c ranged from -1.11×10^{-3} to -2.71×10^{-4}, with an average of -5.30×10^{-4}.

$$y_t = x_{in} \times exp(-d_c \times T) \tag{7}$$

where y_t is the output based on the applied temperature (T) in the furnace, x_{in} is the initial rock property at room temperature, and d_c is the decay constant.

In rock engineering and engineering geology, using dc can be an effective way to obtain a single comparative durability index for waste rocks. This helps incorporate granite waste into various industries by providing cost-effective insights into crushing and grinding. This approach also facilitates quantifying rock degradation resulting from cyclic and/or incremental thermal loading. However, this approach has limitations in scenarios characterised by non-monotonic rock degradation profiles and by reaching temperature thresholds (T_{max}).

Table 7. Decay functions for different rock properties

Waste Material	Decay function	Initial values (ρ_{d-in} – BWI_{in})	t value	R^2
R1	$\rho_{d-T} = \rho_{d-in} \times exp(-3.95 \times 10^{-5}T)$	2.681 g/cm³	−28.27	0.99
	$n_{e-T} = n_{e-in} \times exp(1.13 \times 10^{-3}T)$	0.35 %	29.32	0.97
	$V_{p-T} = V_{p-in} \times exp(-3.59 \times 10^{-4}T)$	5.06 km/s	−29.18	0.98
	$UCS_T = UCS_{in} \times exp(-4.51 \times 10^{-4}T)$	162.70 MPa	−5.88	0.85
	$BWI_T = BWI_{in} \times exp(-4.16 \times 10^{-4}T)$	17.95 kWh/t	−9.90	0.84
R2	$\rho_{d-T} = \rho_{d-in} \times exp(-2.43 \times 10^{-5}T)$	2.610 g/cm³	−15.18	0.97
	$n_{e-T} = n_{e-in} \times exp(2.15 \times 10^{-3}T)$	0.56 %	20.28	0.90
	$V_{p-T} = V_{p-in} \times exp(-5.29 \times 10^{-4}T)$	4.11km/s	−8.61	0.93
	$UCS_T = UCS_{in} \times exp(-4.87 \times 10^{-4}T)$	145.20 MPa	−6.14	0.88
	$BWI_T = BWI_{in} \times exp(-2.71 \times 10^{-4}T)$	16.25 kWh/t	−14.11	0.98
R3	$\rho_{d-T} = \rho_{d-in} \times exp(-4.56 \times 10^{-5}T)$	2.570 g/cm³	−6.42	0.89
	$n_{e-T} = n_{e-in} \times exp(1.31 \times 10^{-3}T)$	1.07 %	23.18	0.97
	$V_{p-T} = V_{p-in} \times exp(-2.94 \times 10^{-4}T)$	4.39 km/s	−7.29	0.92
	$UCS_T = UCS_{in} \times exp(-3.29 \times 10^{-4}T)$	138.40 MPa	−4.78	0.85
	$BWI_T = BWI_{in} \times exp(-5.44 \times 10^{-4}T)$	15.69 kWh/t	14.74	0.96
R4	$\rho_{d-T} = \rho_{d-in} \times exp(-5.44 \times 10^{-5}T)$	2.70 g/cm³	−5.91	0.86
	$n_{e-T} = n_{e-in} \times exp(1.44 \times 10^{-3}T)$	0.76 %	23.22	0.97
	$V_{p-T} = V_{p-in} \times exp(-7.71 \times 10^{-4}T)$	4.28 km/s	−8.51	0.94
	$UCS_T = UCS_{in} \times exp(-4.10 \times 10^{-4}T)$	144.32 MPa	−10.82	0.96
	$BWI_T = BWI_{in} \times exp(-2.81 \times 10^{-4}T)$	17.90 kWh/t	−23.22	0.99
R5	$\rho_{d-T} = \rho_{d-in} \times exp(-4.48 \times 10^{-5}T)$	2.74 g/cm³	−5.40	0.84
	$n_{e-T} = n_{e-in} \times exp(1.80 \times 10^{-3}T)$	0.52 %	16.51	0.96
	$V_{p-T} = V_{p-in} \times exp(-6.26 \times 10^{-4}T)$	5.37 km/s	−19.68	0.96
	$UCS_T = UCS_{in} \times exp(-5.34 \times 10^{-4}T)$	189.17 MPa	−10.36	0.85
	$BWI_T = BWI_{in} \times exp(-5.30 \times 10^{-4}T)$	21.66 kWh/t	−13.77	0.96
R6	$\rho_{d-T} = \rho_{d-in} \times exp(-4.42 \times 10^{-5}T)$	2.680 g/cm³	−8.54	0.85
	$n_{e-T} = n_{e-in} \times exp(2.44 \times 10^{-3}T)$	0.65 %	24.15	0.93
	$V_{p-T} = V_{p-in} \times exp(-5.46 \times 10^{-4}T)$	4.32 km/s	−6.93	0.89
	$UCS_T = UCS_{in} \times exp(-7.53 \times 10^{-4}T)$	109.37 MPa	−14.20	0.96
	$BWI_T = BWI_{in} \times exp(-5.56 \times 10^{-4}T)$	17.85 kWh/t	−29.10	0.98
R7	$\rho_{d-T} = \rho_{d-in} \times exp(-7.74 \times 10^{-5}T)$	2.611 g/cm³	−9.10	0.87
	$n_{e-T} = n_{e-in} \times exp(3.13 \times 10^{-3}T)$	0.88 %	185.2	0.99
	$V_{p-T} = V_{p-in} \times exp(-6.08 \times 10^{-4}T)$	3.96 km/s	−27.14	0.99
	$UCS_T = UCS_{in} \times exp(-1.27 \times 10^{-3}T)$	70.90 MPa	−13.06	0.92
	$BWI_T = BWI_{in} \times exp(-1.11 \times 10^{-3}T)$	14.62 kWh/t	−20.94	0.98

Explanations: ρ_{d-T} – BWI_T: Temperature-dependent outputs, T: Applied temperature in furnace (°C), ρ_{d-in} – BWI_{in}: Initial rock properties at room temperature (~ 25°C), t: Statistical t-value, R^2: Coefficient of determination

In the context of sustainable mineral processing, optimising a granite waste grinding circuit requires a clear understanding of feed material variability to balance throughput, product fineness, and specific energy consumption (Pavloudakis et al. 2024). Specifically, variations in BWI must be precisely quantified to dynamically adjust operational parameters, thereby ensuring the target particle size distribution is achieved with minimal energy consumption. Therefore, the following section presents detailed regression and soft-computing analyses to develop predictive models for assessing BWI as a function of selected rock properties.

4.4. Regression and soft computing analyses

To understand variations in granite quarry waste and its processing for sustainable industrial applications, accurately determining material grindability is essential. In this context, BWI serves as the standard parameter for quantifying the resistance of materials to grinding in a ball mill. However, its direct laboratory measurement is extremely time-consuming and equipment-intensive. To overcome these limitations, predictive modelling based on more repeatable test methods has emerged as a highly efficient alternative.

Traditional statistical approaches, such as multiple linear and nonlinear regression analyses, provide straightforward empirical equations; however, soft computing methods offer advanced, nonlinear capabilities that can capture the more complex, noisy, and heterogeneous nature of rock waste materials (Herrera et al. 2023; Sree and Kanmani 2024). In this section, the BWI of granite waste materials was modelled using regression and soft computing analyses.

4.4.1. Regression analyses

Before developing predictive models, it is useful to examine relationships between the inputs (T, ρ_d, n_e, V_p, and UCS) and the output (BWI). Table 8 summarises these relationships. According to Landis and Koch (1977), T is moderately correlated with BWI (a negative correlation), whereas the other inputs strongly influence BWI.

Based on the correlation analysis results, several simple, multiple, and nonlinear regression analyses were conducted in RStudio 2026. Accordingly, notable predictive models (M1-M6) are presented in Table 9.

Table 8 Pearson's correlation analysis results.

Parameter	T	ρ_d	n_e	V_p	UCS	BWI
T	1					
ρ_d	–0.462	1				
n_e	0.586	–0.701	1			
V_p	–0.668	0.621	–0.722	1		
UCS	–0.367	0.626	–0.755	0.738	1	
BWI	–0.491	0.889	–0.798	0.706	0.827	1

Table 9. Regression analysis results

Model No	Empirical equation	Error metric	
		R^2	RMSE
M1	$BWI = 18.60 - 0.00053T - 2.319n_e$	0.62	1.786
M2	$BWI = -58.91 - 0.00024T + 28.79\rho_d - 1.047n_e$	0.85	1.145
M3	$BWI = 12.08 - 0.00148T - 0.992n_e + 0.041UCS$	0.74	1.452
M4	$BWI = 0.033 \times T^{-0.024} \times {\rho_d}^{6.481}$	0.79	1.305
M5	$BWI = 2.84 \times T^{-0.040} \times UCS^{0.398}$	0.72	1.554
M6	$BWI = 0.074 \times T^{-0.01} \times \rho_d^{5.573} \times n_e^{-0.068}$	0.82	1.243

Based on the regression results summarised in Table 9, the predictive performance of the six models (M1–M6) varies significantly when different input combinations are considered. Among the multiple linear regression models, M2 exhibits the strongest predictive performance, yielding a coefficient of determination (R^2) of 0.85 and an RMSE of 1.145. These statistics indicate that M2 explains approximately 85% of the variability in BWI values. In addition, the non-linear power model (M6) provides a comparably robust fit (R^2 =0.82; RMSE= 1.243) and may be considered as another suitable predictive tool for estimating the BWI of granite waste materials. Notably, both M2 and M6 incorporate the same set of inputs (T, ρ_d, and n_e), suggesting that this combination is effective for modelling BWI.

4.4.2. Soft computing analyses

In mining engineering and earth sciences, interpretable machine learning models connect data analysis with geomechanical and mineral processing challenges. They provide physical consistency, spatial transparency, and diagnostic insights essential for safe and sustainable operations.

In this study, to simplify computation and produce practically applicable mathematical formulations, the multivariate adaptive regression splines (MARS) method, a user-friendly soft computing technique, is used to develop predictive models that are more accurate than those in Table

9. Originally proposed by Friedman (1991), MARS is a semi-parametric regression technique that combines the interpretability of linear modelling with the flexibility of non-parametric methods.

In recent years, MARS has been widely applied to prediction and optimisation problems (Qureshi et al., 2022; Naser et al., 2022; Rana et al., 2025; Eskandarinejad et al., 2025). The method consists of two stages: a forward pass, in which basis functions (BFs) are introduced to capture non-linearities and interactions, and a backward pass, in which these BFs are combined linearly. In this study, MARS-based soft-computing analyses were implemented in RStudio (2026). A 5-fold cross-validation strategy was employed to minimise overfitting risks during soft computing modelling. This means the dataset (Table 3, n=49) was randomly divided into five parts: four with 10 samples and the remaining one with 9. In each round, four parts (39 or 40 samples) were used to train the model, and the remaining part (10 or 9 samples) was used to test it (Fig. 9). Based on the above identification, soft computing modelling was performed as an exploratory exercise. Because the observations and laboratory test results come from seven source materials (R1–R7), measurements of the same material at different temperatures might not be fully independent. Overlooking this dependence could lead to an overestimation of predictive performance. Therefore, when selecting inputs for MARS models, special care was taken to avoid highly correlated pairs (Table 10).

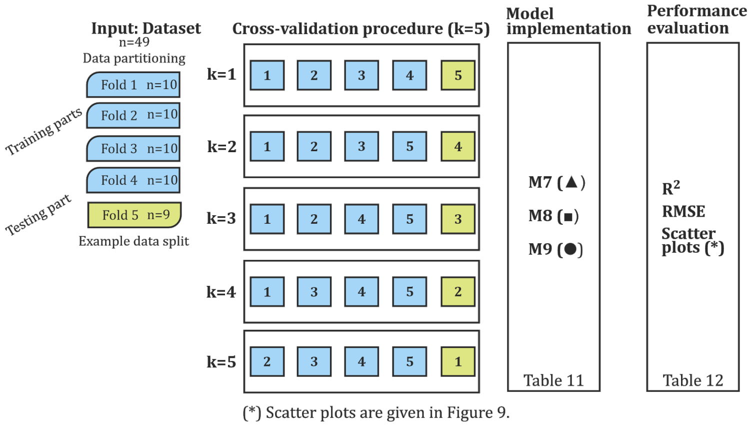

Fig 9. 5-fold cross-validation procedure

Table 10. Input parameters considered in MARS analyses

Model No	Input parameters	Output
M7	T, ρ_d, n_e	
M8	T, n_e, V_p	BWI
M9	T, ρ_d, UCS	

Accordingly, three robust predictive models (M7-M9) were developed to estimate BWI values. The mathematical equations of the established models are listed in Table 11. The performance of these models was evaluated using scatter plots (Fig. 10) and several statistical indicators, including the coefficient of determination (R^2) and the root mean squared error (RMSE) (Table 12). Accordingly, the R^2 and RMSE values range from 0.85 to 0.96 and from 0.60 to 1.18, respectively. The statistical indicators show that the M9 model outperforms the other models. The input parameters considered in this model are T, ρd, and UCS, which together provide a good combination for estimating BWI values.

These models can be easily implemented in computational environments such as MATLAB and Python for practical applications. This enables rapid estimation and visualisation of predicted BWI values under different thermal conditions.

This computational flexibility not only makes it easier for researchers and industry professionals to use but also enables integration with larger process-simulation frameworks for rock comminution and energy optimisation. In this context, the present study can be regarded as a case study that establishes the dual significance of (i) quantifying the thermal effects on selected engineering properties of granite waste materials and (ii) establishing a set of data-driven predictive models capable of evaluating their grinding behaviour with reasonable accuracy.

Table 11. Mathematical equations of the developed models

Model No	Predictive model
M7	$\boldsymbol{BWI = 17.57 + 0.0057BF1 + 73.64BF2 - 5.72BF3 - 0.051BF4 + 0.0079BF5 - 0.021BF6}$ $BF1 = max(0; T - 100)$ $BF2 = max(0; \rho d - 2.685)$ $BF3 = max(0; ne - 0.68)$ $BF4 = T \times max(0; 2.685 - \rho d)$ $BF5 = T \times max(0; ne - 0.97)$ $BF6 = T \times max(0; 0.97 - ne)$
M8	$\boldsymbol{BWI = 49.91 - 0.0194BF1 - 28.32BF2 - 18.76BF3 + 26.32BF4 + 8.04BF5 - 0.013BF6}$ $BF1 = max(0; 400 - T)$ $BF2 = max(0; ne - 0.68)$ $BF3 = max(0; 1.96 - ne)$ $BF4 = max(0; ne - 1.96)$ $BF5 = max(0; Vp - 4.43)$ $BF6 = T \times max(0; 1.96 - ne)$
M9	$\boldsymbol{BWI = 14.29 - 0.14BF1 + 0.008BF2 + 0.00009BF3 - 0.16BF4 + 0.34BF5}$ $BF1 = max(0; 74.88 - UCS)$ $BF2 = max(0; 400 - T)$ $BF3 = T \times max(0; UCS - 74.88)$ $BF4 = max(0; 2.685 - \rho d) \times UCS$ $BF5 = max(0; \rho d - 2.685) \times UCS$

Table 12. Performance evaluation of the developed soft computing models

Performance metric: R^2											
Cross-validation steps	k=1		k=2		k=3		k=4		k=5		Average R^2
	Tr	Te	Tr	Te	Tr	Te	Tr	Te	Tr	Te	
M7	0.96	0.93	0.95	0.91	0.92	0.96	0.94	0.96	0.92	0.97	0.94
M8	0.84	0.83	0.81	0.83	0.92	0.78	0.84	0.91	0.85	0.89	0.85
M9	0.97	0.94	0.95	0.96	0.96	0.94	0.98	0.94	0.95	0.96	0.96
Performance metric: RMSE											
Cross-validation steps	k=1		k=2		k=3		k=4		k=5		Average RMSE
	Tr	Te	Tr	Te	Tr	Te	Tr	Te	Tr	Te	
M7	0.56	0.71	0.49	0.88	0.62	0.52	0.61	0.54	0.61	0.52	0.60
M8	1.18	1.16	1.26	1.19	1.02	1.57	1.01	1.29	1.04	1.08	1.18
M9	0.59	0.68	0.63	0.60	0.54	0.74	0.52	0.64	0.69	0.57	0.62
Explanations: Tr: Training dataset Te: Testing dataset											

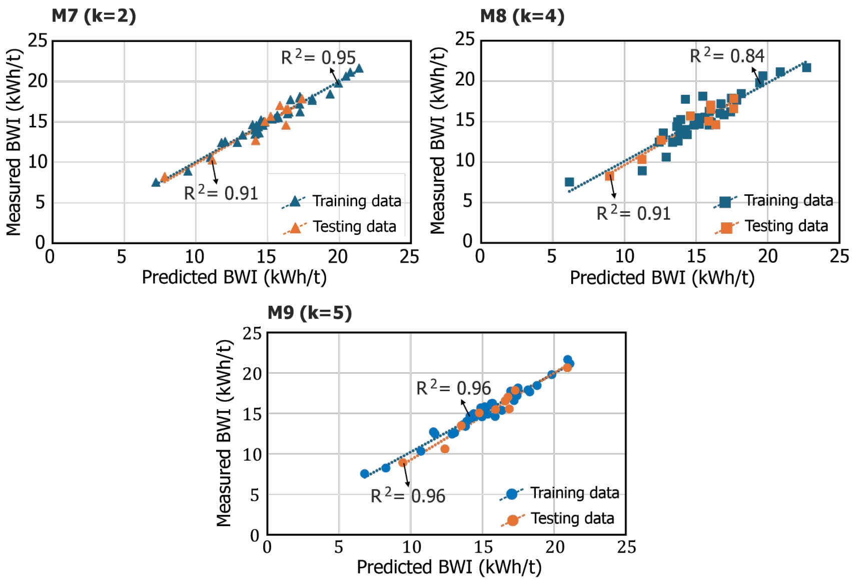

Fig. 10. Scatter plots of the soft computing models in different cross-validation steps

In addition, the industrial relevance of these findings is conditional. A lower BWI after heating indicates improved grindability, but it does not, by itself, demonstrate a net energy benefit, as furnace or microwave energy demand, heat losses, throughput, emission intensity, and equipment costs must be considered.

The present study should therefore be regarded as a laboratory-scale demonstration of potential comminution improvement, forming the basis for subsequent techno-economic and life-cycle analyses rather than as proof of industrial feasibility.

The computational and analytical approaches presented in this work have the potential to promote the efficient use of natural materials and to optimise mineral processing, related geoengineering, and industrial applications.

5. Conclusions

This study examined how the physical, mechanical, and comminution properties of granite waste change under thermal treatment at temperatures up to 600 °C. The laboratory test results indicate a progressive degradation of material properties with increasing temperature, accompanied by improved grindability and crushability. A standard numerical integration approach was used to quantify the thermal quality of the tested wastes; the resulting RPs exhibit heterogeneous thermal-quality profiles governed by the individual rock properties. Consequently, assigning a single thermal quality value to granite waste is not scientifically meaningful, and thermal quality is better interpreted either on a property-by-property basis or through a weighted evaluation. Variations in BWI were further addressed through regression and soft computing analyses; among the nine formulations developed (M1–M9), M9 yielded the best predictive performance, with an R^2 of 0.96 and an RMSE of 0.62.

Thermally assisted comminution of granite waste is industrially viable only if downstream energy savings exceed the cost of thermal pre-treatment. Given the structural limitations of this study, namely the limited sample size, the absence of microstructural imaging, and the lack of independent techno-economic validation, the proposed models are not recommended for direct use in mineral processing design. Future work should therefore combine expanded laboratory testing with comprehensive economic analysis to determine whether thermal pre-treatment offers a net economic benefit.

Acknowledgement

The authors are indebted to anonymous reviewers whose comments and suggestions improved the manuscript.

ABBREVIATION LIST	
A_0: Area in baseline	R^2: Coefficient of determination
A_e: Area under response curve	RMSE: Root mean square error
BWI: Bond Work Index (kWh/t)	RP: Rating point in thermal quality quantification
d_c: Decay constant	T: Applied temperature (°C)
F_{80}: Characterised feed size (μm)	t: Statistical t-value
G: Grindability ratio (g/rev)	UCS: Uniaxial compressive strength
K-Keld: Alkali feldspar	V: Volume of the cubical sample (cm^3)
n_e: Effective porosity (%)	V_p: Pulse wave velocity (km/s)
P_{80}: Characterised product size (μm)	W_d: Oven-dried weight (g)
Plg: Plagioclase	W_s: Saturated weight (g)
P_{max}: Maximum rock property in A_0	XRD: X-ray diffraction
PSD: Particle size distribution	Δx: Step size in trapezoidal method
P_{test}: Test sieve size (μm)	ρ_d: Dry density (g/cm^3)
Qtz: Quartz	ρ_w: Density of distilled water (g/cm^3)
r: Pearson's correlation coefficient	

References

ABDDAIM, E., SAKAMI, S., EL HASSNAOUI, A., BOUKHATTEM, L. 2024. *Impact of temperature on chemical, thermo-physical, and mechanical properties of four rock materials for sensible thermal energy storage.* Journal of Energy Storage 89,111602.

ABDELKADER, H. A., AHMED, A. S., HUSSEIN, M. M., YE, H., ZHANG, J. 2022. *An experimental study on geotechnical properties and micro-structure of expansive soil stabilized with waste granite dust.* Sustainability 14(10),6218.

ADEWUYI, S. O., AHMED, H. A., AHMED, H. M. 2020. *Methods of ore pretreatment for comminution energy reduction.* Minerals 10(5),423.

ALZO'UBI, A. K., ALNEASAN, M. 2025. *The impact of moderate thermal fluctuations on dolomite, from strength enhancement to microstructural sensitivity.* Results in Engineering,107679.

AMULYA, G., MOGHAL, A. A. B., ALMAJED, A. 2021. *A state-of-the-art review on suitability of granite dust as a sustainable additive for geotechnical applications.* Crystals 11(12),1526.

ANON. 1979. *Classification of rocks and soils for engineering geological mapping. Part 1, rock and soil materials.* Bulletin of the International Association of Engineering Geology 19,364–37.

ARAL, I. F., BOY, R., DINÇER, A. R. 2021. *Effects of freeze-thawing cycles on the physical and mechanical properties of basaltic and dolomitic rocks evaluated with a decay function model.* Bulletin of Engineering Geology and the Environment 80(4),2955–2962.

ARAS, A. 2009. *Correlation of mechanical properties of some rocks with their grindability (in Turkish).* PhD dissertation, Selçuk University, Konya, Türkiye.

ARAS, A., ÖZŞEN, H., DURSUN, E. A. 2020. *Using artificial neural networks for the prediction of Bond work index from rock mechanics properties.* Mineral Processing and Extractive Metallurgy Review 41(3),145–152.

ASGARI, K., HUANG, Q., HONAKER, R., SABOLSKY, E. 2024. *Investigating the effect of microwave pretreatment on bastnasite grinding for comminution energy reduction and rare earth recovery.* Processes 12(11),2468.

ASLANNEZHAD, M., KESHAVARZ, A., KALANTARIASL, A. 2020. *Evaluation of mechanical, chemical, and thermal effects on wellbore stability using different rock failure criteria.* Journal of Natural Gas Science and Engineering 78,103276.

ASTM. 2017. *Standard test method for compressive strength of dimension stone.* ASTM C170/C170M-17. ASTM International.

ASTM. 2009. *Standard test methods for absorption and bulk specific gravity of dimension stone.* ASTM C97/C97M. ASTM International.

ASTM. 2020. *Standard practice for measuring ultrasonic velocity in materials by comparative pulse-echo method.* ASTM E494. ASTM International.

BECATTINI, V., MOTMANS, T., ZAPPONE, A., MADONNA, C., HASELBACHER, A., STEINFELD, A. 2017. *Experimental investigation of the thermal and mechanical stability of rocks for high-temperature thermal-energy storage.* Applied Energy 203,373–389.

BOND, F. C. 1961. *Crushing and grinding calculations.* British Chemical Engineering 6(6),378–385.

CISTERNAS, N., TOBOSQUE, P., SBARBARO, D., MUNNIER, C., KRACHT, W., CARRASCO, C. 2022. *Heating pre-treatment of copper ores and its effects on the Bond work index.* Minerals 12(5),593.

DANISH, A., MOSABERPANAH, M. A., SALIM, M. U., FEDIUK, R., RASHID, M. F., WAQAS, R. M. 2021. *Reusing marble and granite dust as cement replacement in cementitious composites, a review on sustainability benefits and critical challenges.* Journal of Building Engineering 44,102600.

DEERE, D. U., MILLER, R. P. 1966. *Engineering classification and index properties for intact rock.* Springfield, VA, USA, National Technical Information Service, 6–10.

DOU, X., SHI, H., QING, Y., GUO, J., CHENG, L. 2025. *Stability analysis of the surrounding rock of deep underground engineering under the action of thermal-solid coupling.* Buildings 15(9),1500.

ELTWATI, A. S., TARHUNI, F., ELKASEH, A. 2020. *Engineering properties of clayey soil stabilized with waste granite dust.* Journal of Critical Reviews 7(16),794–802.

ESKANDARINEJAD, A., ARELLANO, D., NAZARI, R., NIKOO, M. R. 2025. *Multivariate adaptive regression splines (MARS) analysis and complementary machine learning approaches in predicting earthquake-induced slope displacements.* Earth Science Informatics 18(2),398.

FRIEDMAN, J. H. 1991. *Multivariate adaptive regression splines.* The Annals of Statistics 19(1),1–67.

GAUTAM, P. K., VERMA, A. K., JHA, M. K., SHARMA, P., SINGH, T. N. 2018. *Effect of high temperature on physical and mechanical properties of Jalore granite.* Journal of Applied Geophysics 159,460–474.

GOMAH, M. E., LI, G., OMAR, A. A., ABDEL LATIF, M. L., SUN, C., XU, J. 2024. *Thermal-induced microstructure deterioration of Egyptian granodiorite and associated physico-mechanical responses.* Materials 17(6),1305.

GRIFFITHS, L., HEAP, M. J., BAUD, P., SCHMITTBUHL, J. 2017. *Quantification of microcrack characteristics and implications for stiffness and strength of granite.* International Journal of Rock Mechanics and Mining Sciences 100,138–150.

GUPTA, L. K., VYAS, A. K. 2018. *Impact on mechanical properties of cement sand mortar containing waste granite powder.* Construction and Building Materials 191,155–164.

HAFFEZ, G. S. A. 2012. *Correlation between work index and mechanical properties of some Saudi ores.* Materials Testing 54(2),108–112.

HASSANI, F., NEKOOVAGHT, P. M., GHARIB, N. 2016. *The influence of microwave irradiation on rocks for microwave-assisted underground excavation.* Journal of Rock Mechanics and Geotechnical Engineering 8(1),1–15.

HELGESON, H. C. 1978. *Summary and critique of the thermodynamic properties of rock-forming minerals.* American Journal of Science 278,1–229.

HERRERA, N., SINCHE GONZALEZ, M., OKKONEN, J., MOLLEHUARA, R. 2023. *Soft computing application in mining, mineral processing and metallurgy with an approach to using it in mineral waste disposal.* Minerals 13(11),1450.

HUANG, C., ZHU, C., MA, Y. 2025. *Investigating mechanical characteristics of rocks under freeze–thaw cycles using grain-based model.* Rock Mechanics and Rock Engineering 58(1),603–622.

JAMSHIDI, A., NIKUDEL, M. R., KHAMEHCHIYAN, M. 2013. *Predicting the long-term durability of building stones against freeze–thaw using a decay function model.* Cold Regions Science and Technology 92,29–36.

JIN, J., LIU, J., CHEN, W., LI, G., CHENG, W., ZHANG, X., LUO, Y. 2024. *The impact of high temperature on mechanical properties and behaviors of sandstone.* Frontiers in Earth Science 12,1322495.

KAHRAMAN, E. 2022. *Investigation of the effects of two different cooling treatments on the physico-mechanical and microstructural properties of granite after high temperatures.* Geomechanics and Geophysics for Geo-Energy and Geo-Resources 8,142.

KAHRAMAN, S., CANPOLAT, A. N., FENER, M. 2020. *The influence of microwave treatment on the compressive and tensile strength of igneous rocks.* International Journal of Rock Mechanics and Mining Sciences 129,104303.

KINGMAN, S. W., VORSTER, W., ROWSON, N. A. 2000. *The influence of mineralogy on microwave assisted grinding.* Minerals Engineering 13(3),313–327.

KUMARI, W., BEAUMONT, D., RANJITH, P., PERERA, M., ISAKA, B. A., KHANDELWAL, M. 2019. *An experimental study on tensile characteristics of granite rocks exposed to different high temperature treatments.* Geomechanics and Geophysics for Geo-Energy and Geo-Resources 5(1),47–64.

KUMARI, W. G. P., RANJITH, P. G., PERERA, M. S. A., SHAO, S., CHEN, B. K., LASHIN, A., …, RATHNAWEERA, T. D. 2017. *Mechanical behaviour of Australian Strathbogie granite under in-situ stress and temperature conditions, an application to geothermal energy extraction.* Geothermics 65,44–59.

LANDIS JR., KOCH, G. G. 1977. *The measurement of observer agreement for categorical data.* Biometrics 33(1),159–174.

LE PAPE, Y., ALSAID, M. H., GIORLA, A. B. 2018. *Rock-forming minerals radiation-induced volumetric expansion–revisiting literature data.* Journal of Advanced Concrete Technology 16(5),191–209.

LASHEEN, E. S. R., RASHWAN, M. A., AZER, M. K. 2023. *Effect of mineralogical variations on physico-mechanical and thermal properties of granitic rocks.* Scientific Reports 13(1),10320.

LI, J., LI, H., ZHU, Z., TAO, Y., TANG, C. A. 2021. *Numerical study on damage zones induced by excavation and ventilation in a high-temperature tunnel at depth.* Energies 14(16),4773.

LIN, W. 2002. *Permanent strain of thermal expansion and thermally induced microcracking in Inada granite.* Journal of Geophysical Research, Solid Earth 107(B10).

LIU, X., YUAN, S., SIEFFERT, Y., FITYUS, S., BUZZI, O. 2016. *Changes in mineralogy, microstructure, compressive strength and intrinsic permeability of two sedimentary rocks subjected to high-temperature heating.* Rock Mechanics and Rock Engineering 49(8),2985–2998.

LU, J., LI, Y., ZOU, C., LIU, Z., WANG, C. 2019. *Effect of heating rate on the sinterability, crystallization, and mechanical properties of sintered glass–ceramics from granite waste.* Journal of Thermal Analysis and Calorimetry 135,1977–1985.

MEDINA, G., DEL BOSQUE, I. S., FRÍAS, M., DE ROJAS, M. S., MEDINA, C. 2017. *Granite quarry waste as a future eco-efficient supplementary cementitious material (SCM), scientific and technical considerations.* Journal of Cleaner Production 148,467–476.

METSO. 2011. *Crushing and screening handbook.* 6th ed., ed. Keijo Viilo. Tampere, Finland.

MOTLAGH, P. N. 2015. *Physical and mechanical properties of rocks exposed to microwave irradiation, potential application to tunnel boring.* Dissertation, McGill University.

MUTLUTÜRK, M., ALTINDAG, R., TÜRK, G. 2004. *A decay function model for the integrity loss of rock when subjected to recurrent cycles of freezing–thawing and heating–cooling.* International Journal of Rock Mechanics and Mining Sciences 41(2),237–244.

NASER, A. H., BADR, A. H., HENEDY, S. N., OSTROWSKI, K. A., IMRAN, H. 2022. *Application of multivariate adaptive regression splines (MARS) approach in prediction of compressive strength of eco-friendly concrete.* Case Studies in Construction Materials 17,e01262.

NEJATI, H. 2014. *Analysis of physical properties and thermo–mechanical induced fractures of rocks subjected to microwave radiation.* Dissertation, McGill University.

OMRAN, M., FABRITIUS, T., ELMAHDY, A. M., ABDEL-KHALEK, N. A., GORNOSTAYEV, S. 2015. *Improvement of phosphorus removal from iron ore using combined microwave pretreatment and ultrasonic treatment.* Separation and Purification Technology 156,724–737.

OZGUVEN, A., OZCELIK, Y. 2014. *Effects of high temperature on physico-mechanical properties of Turkish natural building stones.* Engineering Geology 183,127–136.

PAUL, S., CHATTOPADHYAYA, S., RAINA, A. K., SHARMA, S., LI, C., ZHANG, Y., …, TAG-ELDIN, E. 2022. *A review on the impact of high-temperature treatment on the physico-mechanical, dynamic, and thermal properties of granite.* Sustainability 14(22),14839.

PAVLOUDAKIS, F., ROUMPOS, C., SPANIDIS, P. M. 2024. *Sustainable mining and processing of mineral resources.* Sustainability 16(19),8393.

PURWANTO, H., SHIMADA, T., TAKAHASHI, R., YAGI, J. I. 2002. *Lowering of grinding energy and enhancement of agglomerate strength by dehydration of Indonesian laterite ore.* ISIJ International 42(3),243–247.

QURESHI, M. U., MAHMOOD, Z., RASOOL, A. M. 2022. *Using multivariate adaptive regression splines to develop relationship between rock quality designation and permeability.* Journal of Rock Mechanics and Geotechnical Engineering 14(4),1180–1187.

RAGHAVENDRA, R., SHARADA, S. A., RAVINDRA, M. V. 2015. *Compressive strength of high-performance concrete using granite powder as fine aggregate.* International Journal of Research in Engineering and Technology 4,47–49.

RAM, B. K., DAS, R., MISHRA, D. A. 2025. *Thermal treatment induced damage mechanism of rock materials and its influence on the physico-mechanical properties, a review.* Environmental Earth Sciences 84(12),334.

RAMADJI, C., MESSAN, A., PRUD'HOMME, E. 2020. *Influence of granite powder on physico-mechanical and durability properties of mortar.* Materials 13(23),5406.

RANA, A., SINGH, A., KOMADJA, G. C., AGRAWAL, H., SINGH, R. K. 2025. *Application of multivariate adaptive regression splines technique for blast-induced air overpressure control in mines using large dataset.* Noise Control Engineering Journal 73(1),38–56.

RANJBAR, A., MOUSAVI, A., ASGHARI, O. 2021. *Using rock geomechanical characteristics to estimate Bond work index for mining production blocks.* Mining, Metallurgy & Exploration 38(6),2569–2583.

RANJITH, P., VIETE, D. R., CHEN, B. J., PERERA, M. S. A. 2012. *Transformation plasticity and the effect of temperature on the mechanical behaviour of Hawkesbury sandstone at atmospheric pressure.* Engineering Geology 151,120–127.

RAO, R. B., VEERESH, M. B., BANERJEE, G. N. 2002. *Effect of thermal pretreatment on grindability and upgradation of bauxite for refractory applications.* Light Metals, Proceedings of Sessions, TMS Annual Meeting, 205–208. Warrendale, Pennsylvania.

RONG, G., PENG, J., YAO, M., JIANG, Q., WONG, L. N. Y. 2018. *Effects of specimen size and thermal-damage on physical and mechanical behavior of a fine-grained marble.* Engineering Geology 232,46–55.

SHAH, S. H. A., HABIB, U., MOHAMED, A., AZIZ, M., REHMAN, Q. U., SALEEM, A. 2022. *Laboratory and in situ stabilization of compacted clay through granite waste powder.* Sustainability 14(21),14459.

SIEGESMUND, S., SOUSA, L., KNELL, C. 2018. *Thermal expansion of granitoids.* Environmental Earth Sciences 77(2),41.

SILVA, M. B., HERMO, B. S., GARCÍA-RODEJA, E., FREIRE, N. V. 2005. *Reutilization of granite powder as an amendment and fertilizer for acid soils.* Chemosphere 61(7),993–1002.

SINGH, V., DIXIT, P., VENUGOPAL, R., VENKATESH, K. B. 2019. *Ore pretreatment methods for grinding, journey and prospects.* Mineral Processing and Extractive Metallurgy Review 40(1),1–15.

SOMANI, A., NANDI, T. K., PAL, S. K., MAJUMDER, A. K. 2017. *Pre-treatment of rocks prior to comminution–a critical review of present practices.* International Journal of Mining Science and Technology 27(2),339–348.

SOOSAN, T. G., SRIDHARAN, A., JOSE, B. T., ABRAHAM, B. M. 2005. *Utilization of quarry dust to improve the geotechnical properties of soils in highway construction.* Geotechnical Testing Journal 28(4),391–400.

SREE, T. R., KANMANI, S. 2024. *A comprehensive review of the role of soft computing techniques in municipal solid waste management.* Environmental Technology Reviews 13(1),168–185.

STRZAŁKOWSKI, P., DUCHNOWSKA, M., BAKALARZ, A., GUZIK, K., RATAJCZAK, T., KAŹMIERCZAK, U., GALOS, K. 2025. *Properties of fine-grained rock waste from the production of granite elements in the Strzegom region, Poland – a case study.* Physicochemical Problems of Mineral Processing 61(2),204398.

TAWFIK, M. E., ESKANDER, S. B., AHMED, N. M. 2022. *Potential applications of granite waste powder as an add-value polymer composite product.* Polymers and Polymer Composites 30,1–13.

TCHADJIÉ, L. N., DJOBO, J. N. Y., RANJBAR, N., TCHAKOUTÉ, H. K., KENNE, B. D., ELIMBI, A., NJOPWOUO, D. 2016. *Potential of using granite waste as raw material for geopolymer synthesis.* Ceramics International 42(2),3046–3055.

TIAN, H., MEI, G., JIANG, G. S., QIN, Y. 2017. *High-temperature influence on mechanical properties of diorite.* Rock Mechanics and Rock Engineering 50,1661–1666.

TOMÁS, R., CANO, M., PULGARÍN, L. F., BROTÓNS, V., BENAVENTE, D., MİRANDA, T., VASCONCELOS, G. 2021. *Thermal effect of high temperatures on the physical and mechanical properties of a granite used in UNESCO World Heritage sites in north Portugal.* Journal of Building Engineering 43,102823.

VIDANA PATHIRANAGEI, S., GRATCHEV, I., KONG, R. 2021. *Engineering properties of four different rocks after heat treatment.* Geomechanics and Geophysics for Geo-Energy and Geo-Resources 7,1–21.

VISHAL, V., PRADHAN, S. P., SINGH, T. N. 2011. *Tensile strength of rock under elevated temperatures.* Geotechnical and Geological Engineering 29,1127–1133.

WANG, F., FRUHWIRT, T., KONIETZKY, H. 2020. *Influence of repeated heating on physical-mechanical properties and damage evolution of granite.* International Journal of Rock Mechanics & Mining Sciences 136,104514.

WU, Q., WENG, L., ZHAO, Y., GUO, B., LUO, T. 2019. *On the tensile mechanical characteristics of fine-grained granite after heating/cooling treatments with different cooling rates.* Engineering Geology 253,94–110.

XIAO, Z. Y., XU, W. 2019. *Assessment of strength development in cemented coastal silt admixed granite powder.* Construction and Building Materials 206,470–482.

XU, Z., WU, C., YU, M., LIU, C., QI, W., LIU, L. 2025. *Static mechanical properties of rock–concrete composite specimens after high-temperature treatment.* Rock Mechanics and Rock Engineering,1–25.

YANG, Z., TAO, M., MEMON, M. B., ZHUANG, D., ZHAO, Y. 2025. *Microwave irradiation-induced deterioration of rock mechanical properties and implications for mechanized hard rock excavation.* Journal of Rock Mechanics and Geotechnical Engineering 17(1),275–290.

YIN, T., CHEN, Y., LI, X., LI, Q. 2021. *Effect of high temperature and strain rate on the elastic modulus of rocks, a review.* International Journal of Earth Sciences 110(8),2639–2660.

ZAFAR, M. S., JAVED, U., KHUSHNOOD, R. A., NAWAZ, A., ZAFAR, T. 2020. *Sustainable incorporation of waste granite dust as partial replacement of sand in autoclave aerated concrete.* Construction and Building Materials 250,118878.

ZARAISKY, G. P., BALASHOV, V. N. 1994. *Thermal decompaction of rocks.* In, *Fluids in the crust, equilibrium and transport properties*, 253–284. Dordrecht, Springer Netherlands.

ZHANG, Y., ZHAO, G. F. 2020. *A global review of deep geothermal energy exploration, from a view of rock mechanics and engineering.* Geomechanics and Geophysics for Geo-Energy and Geo-Resources 6(1),4.

ZHANG, L., MAO, X., LU, A. 2009. *Experimental study on the mechanical properties of rocks at high temperature.* Science in China Series E, Technological Sciences 52(3),641–646.

ZHANG, W., SUN, Q., HAO, S., GENG, J., LV, C. 2016. *Experimental study on the variation of physical and mechanical properties of rock after high temperature treatment.* Applied Thermal Engineering 98,1297–1304.

ZHANG, Y., ZHANG, F., YANG, K., CAI, Z. 2022. *Effects of real-time high temperature and loading rate on deformation and strength behavior of granite.* Geofluid,9426378.

ZHENG, L., LI, D., XU, S. 2021. *Analysis on the impact crushing dust generation test method and its influencing factors.* Powder Technology 388,100–109.

ZHU, Z., TIAN, H., JIANG, G., DOU, B. 2022. *Effects of high temperature on rock bulk density.* Geomechanics and Geoengineering 17(2),647–657.